International Journal of Modern Physics C
Vol. 27, No. 5 (2016) 1650048 (14 pages)

DOI: 10.1142/S0129183116500480

World Scientific
www.worldscientific.com

Influence of periodic traffic congestion on epidemic spreading

Muhua Zheng*

Department of Physics
East China Normal University
Shanghai 200062, P. R. China
zhengmuhua163@gmail.com

Zhongyuan Ruan

Center for Network Science
Central European University, Nador u. 9
1051 Budapest, Hungary

Ming Tang

Web Science Center
University of Electronic Science and Technology of China
Chengdu 611731, P. R. China

Younghae Do

Department of Mathematics
Kyungpook National University
Daegu 702-701, South Korea

Zonghua Liu

Department of Physics
East China Normal University
Shanghai 200062, P. R. China
zhliu@phy.ecnu.edu.cn

Received 8 March 2015
Accepted 6 October 2015
Published 27 November 2015

In the metropolis, traffic congestion has become a very serious problem, especially in rush hours. This congestion causes people to have more chance to contact each other and thus will accelerate epidemic spreading. To explain this observation, we present a reaction–diffusion (RD) model with a periodic varying diffusion rate to represent the daily traveling behaviors of human beings and its influence to epidemic spreading. By extensive numerical simulations, we find that the epidemic spreading can be significantly influenced by traffic congestion where the amplitude, period and duration of diffusion rate are the three key parameters. Furthermore, a brief theory is presented to explain the effects of the three key parameters. These findings suggest that except

*Corresponding author.

the normal ways of controlling contagion in working places and long-distance traveling, controlling the contagion in daily traffic congestion may be another effective way to reduce epidemic spreading.

Keywords: Epidemic spreading; complex network; traffic congestion.

PACS Nos.: 89.75.Hc, 87.23.Ge, 87.19.X-, 05.70.Fh.

1. Introduction

The modern society is becoming more and more fast-paced, which guarantees the fast growth of the economy. To get a higher payoff, people frequently change their jobs and thus resulting in a separation between their homes and working places. In cities especially metropolis, people generally go to office in the morning and back to home in the evening, which results in a synchronized pace, called rush hours. A serious consequence of rush hours is the traffic congestion in which haste brings no success. This phenomenon has been observed for a long time and recently been treated as a Bose–Einstein condensation (BEC) of agents in complex networks.[1–4] It is found that network topology is an important factor to influence the condensation. On the other hand, this problem has been also investigated in communication in Internet where the main concentration is how to reduce the traffic congestion by designing efficient algorithms.[5–14] In all these studies, no matter it is BEC or communication in Internet, the diffusion rates at different nodes can be different but they are considered as constants, once fixed, i.e. not varying with time.

However, in the situation of realistic traffic, the diffusion rates have to depend on time, which is the characteristic feature of human activities.[15] Based on the observations that there are both daily and weekly traffic cycles, it is necessary to consider the case of periodic varying diffusion rate. Thus, in this contribution, we present a reaction–diffusion (RD) model with a periodic varying diffusion rate to describe the daily traveling behaviors of human beings.

A hot topic closely related to traffic congestion is epidemic spreading. In the congestion process, people will stay in some common places such as subways, buses, cars, train stations or airports for longer time and thus will have more chance to contact each other. As viruses are spreading through mediums such as body-contact or air and the contagion is proportional to the contact time,[16] the congestion process definitely results in epidemic spreading. To understand its underlying mechanism, much attention has been recently paid to the influence of traffic on epidemic spreading. For example, in email exchange networks,[17] it was found that computer viruses by non-Poisson nature of the contact dynamics decay much slower than predicted by the standard Poisson-process-based models. In transportation networks, the influence of network topology was considered in Refs. 18–21 and the reaction at links was considered in Ref. 22. In traffic-driven epidemic spreading, it was found that the value of the epidemic threshold depends directly on flow conditions,[23–25] etc. These works significantly increase our understanding on epidemic

spreading by human dynamics. However, there is no work so far on how the periodic rush hours of daily travel influences epidemic spreading, which is in fact one of the main ways to spread viruses. Thus, we address this problem in this paper. By extensive numerical simulations, we find that the epidemic spreading can be significantly influenced by traffic congestion where the amplitude, period and duration of diffusion rate are the three key parameters. Then, we give a brief theory to explain the effects of the three parameters.

The rest of this paper is organized as follows. In Sec. 2, we present a model to discuss the influence of traffic congestion on epidemic spreading. Then in Sec. 3, we make numerical simulations to show the effects of the three key parameters. After that, we give a brief theoretical analysis to the obtained numerical results in Sec. 4. Finally, we give discussions and conclusions in Sec. 5.

2. Model

There are evidences to show that traffic networks are usually scale-free (SF), including subway, bus and airport networks.[26–29] Thus, we here consider an SF network of the uncorrelated configuration model (UCM) with a power-law degree distribution $P(k) = c_1 k^{-3}$,[30] where the degree k ranges from $k_{\min} = 3$ to $k_{\max} = \sqrt{N}$, $c_1 = 18N/(N-9)$ and N is the size of network. Initially, we distribute totally N_p agents on the N nodes of network by letting the agents on a node with degree k be $n_k(0) = c_2 k$ with $c_2 = N_p/N\langle k\rangle$ and $\langle k\rangle$ being the average degree. Then, we let each agent have a probability to travel and thus the system will begin its evolution and $n_k(0)$ will become $n_k(t)$ at time t. To simulate the traveling of people in the UCM network, we divide the agents at a node into two parts, i.e. travelers $n_k^T(t)$ and nontravelers $n_k^H(t)$ with $n_k(t) = n_k^T(t) + n_k^H(t)$ and $n_k^T(t)$ coming from the k neighboring nodes. The travelers can be generated from the nontravelers at each time step by a probability p, thus the new travelers generated at a node at time t will be $pn_k^H(t)$. Once an agent is chosen to be a new traveler, a destination will be given preferentially from the remaining $N-1$ nodes of the network by a probability proportional to their degrees. This objective traveling will make each traveler go along the shortest path to arrive its destination, in contrast to the random diffusion where a traveler may randomly choose one of its neighbors as the destination. We use the algorithm given in Refs. 10 and 14 to implement the shortest path. Each traveler will go one step forward along the shortest path at each time step, if the traffic is in the free phase; otherwise, it will queue in the line according to the first-in-first-out policy. Let d_{ij} be the shortest distance between the nodes i and j, a traveler will take at least d_{ij} steps to move from its starting node i to its destination node j. Once the traveler arrives its destination, it will become a nontraveler. Thus, the travelers at a node include both the passing by travelers and the newly generated ones, while the nontravelers include both the remained nontravelers and the new ones arrived their destinations. A simple sketch of the RD model with a periodic varying diffusion rate is represented in Fig. 1.

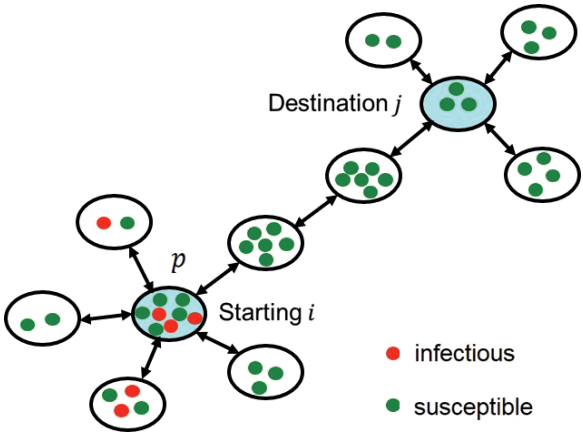

Fig. 1. (Color online) Schematic illustration of the RD model with a periodic varying diffusion rate. The circles represent the nodes and the lines with arrow denote the links between two neighboring nodes. The agents are indicated by different colored dots in the picture. In node i, an agent can travel with rate varying diffusion rate p from starting node i to destination j following the shortest path in the network. If the traffic is in the free phase, this agent will take at least three steps to its destination node j. However, if a traffic congestion occur, the time to the destination node j will be longer than three steps.

Because of the limitations of road's width and subway frequency etc, each node will have a finite capacity to transfer travelers. We let the capacity be $E_k = \beta n_k(0)$, i.e. a node with degree k can deliver at most E_k agents at each time step, which is similar to the communication capacity in Internet.[10,14] A larger β means a larger delivering ability. Let $Q_i^{\text{out}}(t)$ be the delivered agents of node i at time t and $Q_i^{\text{in}}(t)$ be the travelers waiting to leave. We have $Q_i^{\text{in}}(t) = n_k^T(t) + pn_k^H(t)$. At the same time, we have $Q_i^{\text{out}}(t) = Q_i^{\text{in}}(t)$ when $Q_i^{\text{in}}(t) < E_k$ and $Q_i^{\text{out}}(t) = E_k$ when $Q_i^{\text{in}}(t) > E_k$, indicating that travelers will be accumulated once $Q_i^{\text{in}}(t) > E_k$. A traffic congestion will occur provided that the accumulation becomes more and more serious. We introduce an order parameter

$$Q(t) = \frac{1}{N}\sum_{i=1}^{N}(Q_i^{\text{in}}(t) - Q_i^{\text{out}}(t)) \tag{1}$$

to measure the degree of congestion. The system will be in the free phase when $Q(t) = 0$ and congestion phase when $Q(t) > 0$. The larger $Q(t)$ implies a more serious congestion.

The traffic congestion can be also measured by the traveling time. Let $t_s(j)$ be the time for the traveler j to arrive its destination and $t_l(j)$ be the length of its shortest path. Then, we introduce an average time difference

$$\langle \Delta t \rangle = \frac{1}{N_{\text{arrive}}}\sum_{j=1}^{N_{\text{arrive}}}\frac{t_s(j) - t_l(j)}{t_l(j)} \tag{2}$$

to measure the degree of congestion, where N_{arrive} represents the number of travelers arriving their destinations. $\langle \Delta t \rangle$ will be zero in the free phase and greater than zero in the congestion phase.

As pointed out in the introduction, the daily travels of people are periodic with a larger diffusion rate in the rush hours and a smaller diffusion rate in the nonrush hours. To reflect this spatio-temporal feature of human behaviors, we let the traveling probability p be periodic and take the following expression:

$$p(t) = \begin{cases} p_0 + A, & 0 \leq t < T/n \\ p_0 - A/(n-1), & T/n \leq t \leq T \end{cases} \tag{3}$$

where A, T represent the amplitude and period, respectively, and T/n denotes the duration of rush hours. To make $p(t)$ close to realistic situation, we let $p(t)$ satisfy two conditions: (i) $p(t) > 0$, which requires $A < (n-1)p_0$; and (ii) the traveling people in a period of T should be kept a conservation of $p_0 T$, i.e. $\int_0^T p(t)dt = p_0 T$ is independent of the parameters A and n.

We now consider epidemic spreading in the above networked traffic system. We choose the standard susceptible-infected-susceptible (SIS) model,[31–39] where a susceptible agent may be infected with an infectious rate λ if it contacts an infected agent. At the same time, an infected agent may become susceptible automatically with a recovery rate μ. Note that there are multiple agents in every node. The standard SIS model has to be replaced by the RD model[40–42,22,43] where the contagion process is divided into two sub-processes: reaction and diffusion. In the reaction process, all the agents at the same node are assumed to be well-mixed and an infected agent can contact all the other agents at the same node. For convenience, we let $n_k(t) = n_{k,S}(t) + n_{k,I}(t)$ where $n_{k,S}(t)$ and $n_{k,I}(t)$ represent the susceptible and infectious agents in a node with degree k, respectively. Thus, the probability for a susceptible agent to become an infected one is $1 - (1-\lambda)^{n_{i,I}}$ where $n_{i,I}$ represents the number of infected agents at node i. While in the diffusion process, the nontravelers will become travelers by a diffusion rate, i.e. the traveling probability p, and the first E_i travelers in the queue of node i will be moved to their next stations along their shortest paths.

To measure epidemic spreading, we introduce a quantity

$$\rho(t) = \frac{1}{N_p} \sum_{i=1}^{N} n_{i,I} \tag{4}$$

to represent the density of infected agents in steady state. The influence of traffic congestion to epidemic spreading can be reflected by $\rho(t)$.

3. Numerical Simulations

In numerical simulations, we first construct an UCM network with size N and average degree $\langle k \rangle \approx 5$ by the algorithm in Ref. 30. Then, we input $N_p = 100N$ agents to the N nodes of network by letting the agents at node i be $n_i(0) = c_2 k_i$. Before

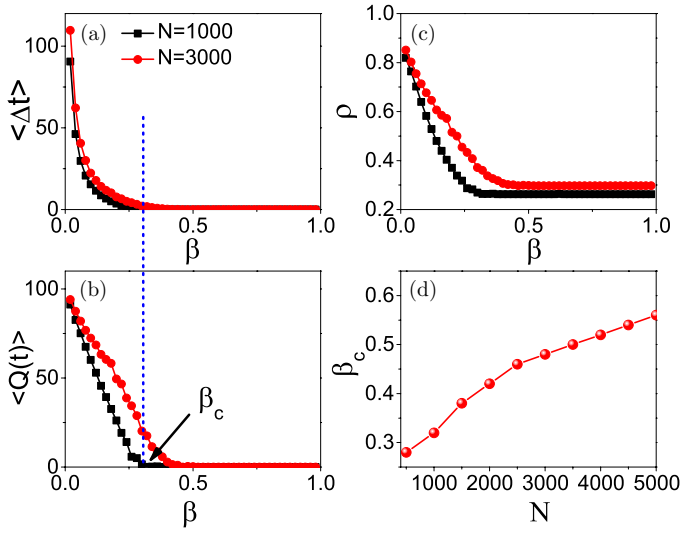

Fig. 2. (Color online) Case of constant diffusion rate with $p = p_0 = 0.02$ where β_c represents the critical point and the averages are obtained by 100 realizations. In (a)–(c), the curves with "squares" and "circles" represent the cases of $N = 1000$ and 3000, respectively, with (a) $\langle \Delta t \rangle$ versus β, (b) $\langle Q(t) \rangle$ versus β, and (c) ρ versus β. The dependence of β_c on the network size is shown in (d).

considering the case of periodic diffusion rate (3), we first try the case of constant diffusion rate with $p = p_0 = 0.02$. Figures 2(a) and 2(b) show the dependence of the order parameter $\langle \Delta t \rangle$ and $\langle Q(t) \rangle$ on the capacity parameter β, respectively, where $\langle Q(t) \rangle$ is the time average of $Q(t)$ in the stabilized state and the two curves with "squares" and "circles" represent the cases of $N = 1000$ and 3000, respectively. It is easy to see that there is a critical $\beta_c = 0.32$ for the case of $N = 1000$ and $\beta_c = 0.46$ for the case of $N = 3000$. Both $\langle \Delta t \rangle$ and $\langle Q(t) \rangle$ are zero for $\beta > \beta_c$ and greater than zero for $\beta < \beta_c$, indicating that the system is congested for $\beta < \beta_c$. To investigate the influence of traffic congestion to epidemic spreading, we fix $\lambda = 0.001$ and $\mu = 0.1$ in this paper and let initially 0.1% people be infected. Figure 2(c) shows the dependence of the density ρ on β. From Fig. 2(c) we see that ρ is a constant for $\beta > \beta_c$ and increases with the decrease of β for $\beta < \beta_c$, indicating that the traffic congestion enhances epidemic spreading. Figure 2(d) shows the dependence of the critical point β_c on the network size. In the following discussions, we fix $N = 1000$ and $N_p = 10^5$, if without specific illustration.

Note that traffic congestion more often happens in a hub node (i.e. a big city) because of its heavy traffic flow and limited capacity (i.e. road width). This phenomenon implies that the capacity β in a metropolis will be close to but smaller than β_c. Thus, we fix $\beta = 0.32$ in the following discussions. We consider the case of Eq. (3) with periodic varying $p(t)$. Figure 3(a) shows the forms of $p(t)$ for different amplitudes A with fixed $T = 240$ and $n = 5$, where the line of $A = 0$ represents the case of constant diffusion rate with $p = p_0 = 0.02$ in Fig. 2. Correspondingly, Figs. 3(b) and

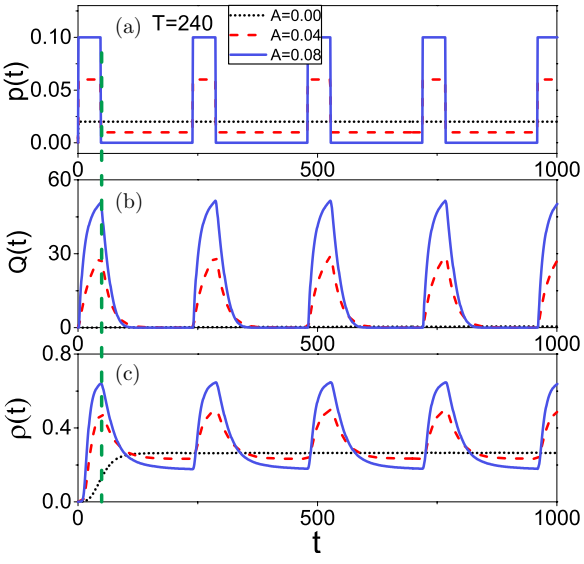

Fig. 3. (Color online) Case of Eq. (3) with periodic varying $p(t)$ and fixed $T = 240$ and $n = 5$, where the curves represent the cases of $A = 0, 0.04$ and 0.08, respectively. (a) $p(t)$ versus t, (b) $Q(t)$ versus t and (c) $\rho(t)$ versus t.

3(c) show the evolutions of $Q(t)$ and $\rho(t)$, respectively. From Fig. 3(b), we see that compared to the case of $A = 0$, the cases of $A > 0$ cause $Q(t) > 0$ and $Q(t)$ is proportional to A, indicating that a congestion phase has been induced by $A > 0$ and the degree of congestion becomes more serious with the increase of A. From Fig. 3(c), we see that the infected fraction $\rho(t)$ will initially increase with t and then quickly reach a steady state. We note that there are two features in Fig. 3(c): (i) The integration of each curve with $A > 0$ is greater than that of $A = 0$, confirming that the traffic congestion has enhanced epidemic spreading. (ii) The dotted line between Figs. 3(a) and 3(c) shows that $\rho(t)$ will continue to be large for a finite time when $p(t)$ drops to its bottom. As the traffic congestion cannot keep smooth immediately when $p(t)$ drops to bottom, the agents still have more chance to contact each other and thus will accelerate epidemic spreading.

To see the influence of the period T, Fig. 4 shows the results of $T = 60$ where the other parameters are kept the same as in Fig. 3. Comparing the corresponding panels between Figs. 3 and 4, it is clear that the values of $Q(t)$ and $\rho(t)$ in Fig. 4 are much smaller than that in Fig. 3, indicating that a larger period T favors the epidemic spreading. Similarly, Fig. 5 shows the influence of the duration parameter of rush hours n where we fix $T = 240$ and $A = 0.02$ and the three curves represent the cases of $n = 2, 5$ and 10, respectively. It is easy to see that the values of $Q(t)$ and $\rho(t)$ are seriously influenced by n, indicating that the duration parameter n is also a key parameter to influence the epidemic spreading. From Fig. 5(c), we see that the fluctuation of $\rho(t)$ decreases with the increase of n. This result can be easily

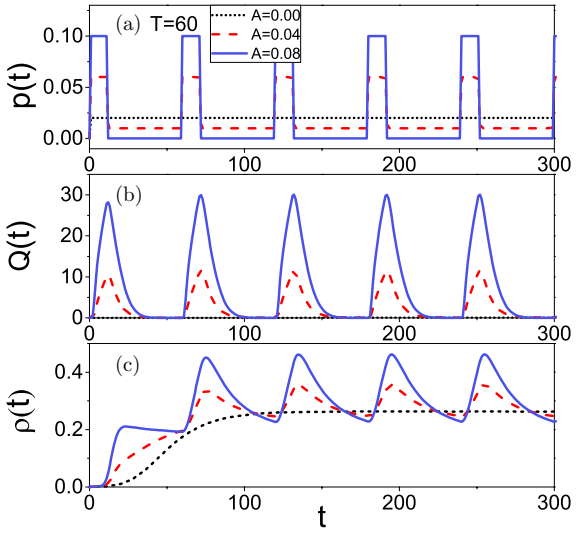

Fig. 4. (Color online) Case of Eq. (3) with periodic varying $p(t)$ and fixed $T = 60$ and $n = 5$, where the curves represent the cases of $A = 0, 0.04$ and 0.08, respectively. (a) $p(t)$ versus t, (b) $Q(t)$ versus t and (c) $\rho(t)$ versus t.

understood because smaller n means longer rush hours and thus results in heavy epidemic spreading.

In sum, we have figured out three key parameters to influence the epidemic spreading, i.e. A, T and n. Note that the panicky behaviors are usually caused by the

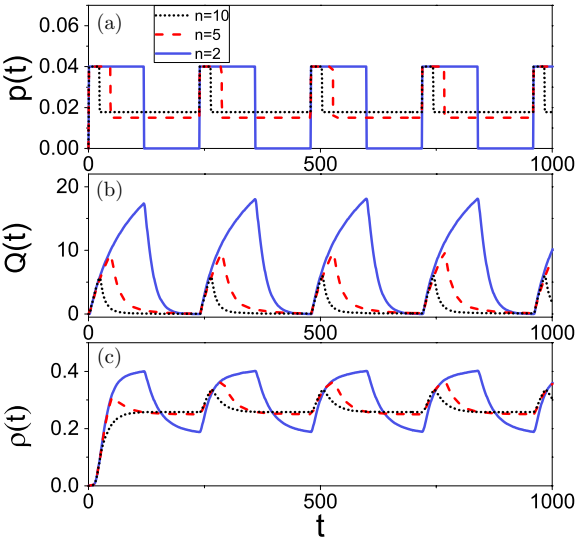

Fig. 5. (Color online) Case of Eq. (3) with periodic varying $p(t)$ and fixed $T = 240$ and $A = 0.02$, where the curves represent the cases of $n = 2, 5$ and 10, respectively. (a) $p(t)$ versus t, (b) $Q(t)$ versus t, and (c) $\rho(t)$ versus t.

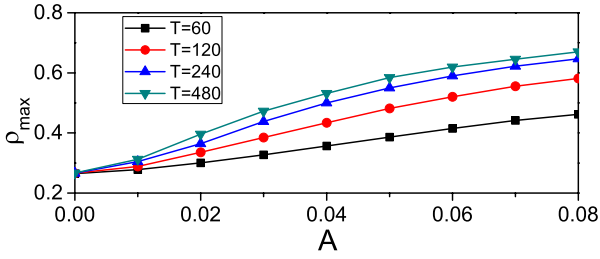

(a)

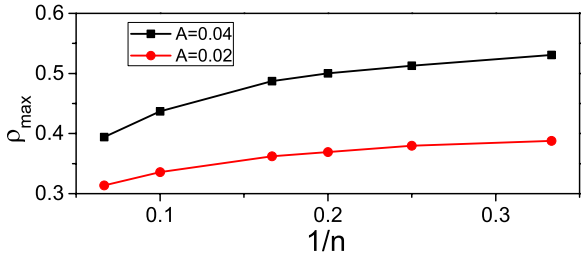

(b)

Fig. 6. (Color online) Dependence of $\rho_{\max}$ on the three key parameters. (a) $\rho_{\max}$ versus A with $n = 5$, where the four curves represent the cases of $T = 60, 120, 240$ and 480, respectively. (b) $\rho_{\max}$ versus $1/n$ with $T = 240$, where the two curves represent the cases of $A = 0.02$ and 0.04, respectively.

possible largest density $\rho_{\max}$, we study how the three key parameters influence $\rho_{\max}$. Figure 6(a) shows the dependence of $\rho_{\max}$ on A, where the four curves represent the cases of $T = 60, 120, 240$ and 480, respectively. We see that $\rho_{\max}$ increases monotonously with both A and T by a nonlinear way. Figure 6(b) shows the dependence of $\rho_{\max}$ on $1/n$, where the two curves represent the cases of $A = 0.02$ and 0.04, respectively. We see that $\rho_{\max}$ also increases with $1/n$ in a nonlinear way.

4. A Brief Theoretical Analysis

To explain the obtained numerical simulations, we here give a brief theoretical analysis. First, we derive the critical point β_c. From Eq. (1), we know that for a given p, the congestion of system is determined by the hub node. The system will be in the free phase when $Q^{\text{in}}_{\text{hub}}(t) < E_{\text{hub}}$ and in the congestion phase when $Q^{\text{in}}_{\text{hub}}(t) > E_{\text{hub}}$, thus we have $Q^{\text{in}}_{\text{hub}}(t) = E_{\text{hub}}$ at the critical point β_c. For a concrete node with degree k, we have the following relationship at the critical point:

$$n_k^T(t) + pn_k^H(t) \leq \beta_c n_k(0), \tag{5}$$

where the relation "=" is only for the hub node and "<" for other nodes. $n_k^T(t)$ and $n_k^H(t)$ satisfy

$$\sum_k NP(k)(n_k^T(t) + n_k^H(t)) = N_p. \tag{6}$$

Let $d \equiv \langle d_{ij} \rangle$ be the average shortest distance. In the steady state, one d-th of the total travelers will arrive their destinations, i.e. $\sum_k NP(k)n_k^T(t)/d$. Considering that the destinations are chosen preferentially by a probability proportional to degree k, we have $\frac{k}{N\langle k \rangle}\sum_k NP(k)n_k^T(t)/d$ agents to arrive at a destination node with degree k at each time step. By the feature of steady state, we have

$$pn_k^H(t) = \frac{k}{N\langle k \rangle}\sum_k NP(k)n_k^T(t)/d. \tag{7}$$

From Eqs. (6) and (7), we obtain $\langle n_k^T(t) \rangle \equiv \sum_k P(k)n_k^T(t) = \frac{pdN_p}{(1+pd)N}$ and thus have

$$n_k^H(t) = \frac{k}{\langle k \rangle}\frac{N_p}{(1+pd)N}. \tag{8}$$

Note that the betweenness $B(k)$ represents how many shortest paths go through a node with degree k,[44] thus statistically, we have

$$n_k^T(t) = \frac{B(k)}{\langle B(k) \rangle}\langle n_k^T(t) \rangle = \frac{B(k)}{\langle B(k) \rangle}\frac{pdN_p}{(1+pd)N}. \tag{9}$$

As the congestion is determined by the hub node with the maximum betweenness, we take $k = k_{\max}$ and substitute Eqs. (8) and (9) into Eq. (5). We obtain

$$\beta_c = \frac{p}{1+pd}\left[1 + \frac{d\langle k \rangle B(k_{\max})}{k_{\max}\langle B(k) \rangle}\right]. \tag{10}$$

Substituting the values of parameters $p = 0.02$, $d = 4.585$, $\langle k \rangle = 5$, $B(k_{\max}) = 0.056359$, $k_{\max} = 23$ and $\langle B(k) \rangle = 0.003593273$ into Eq. (10), we obtain $\beta_c \approx 0.31$, which is very close to the numerical $\beta_c = 0.32$ in Fig. 2. For an uncorrelated SF network with large size N, we have $B(k) \sim k^\eta$, $d \sim \ln N$ and $\eta \approx 1.66$ for $\gamma = 3$.[45,46] When network size N increases, $k_{\max} = \sqrt{N}$ will become larger and $B(k_{\max})/k_{\max}$ will increase. As $\langle k \rangle$ and $\langle B(k) \rangle$ are insensitive with large size N, the threshold value β_c will increase with network size N (see Fig. 2(d)).

We now turn to understand why the traffic congestion can enhance epidemic spreading. To investigate how the three key parameters A, T and n influence epidemic spreading, we focus on the $\rho_{\max}$ in Fig. 6. From Figs. 2 to 4, we note that the moment t_m to obtain $\rho_{\max}$ is approximately the moment to get the maximum congestion $Q(t)$, thus it is interesting to see the distribution of agents at t_m. Figure 7(a) shows the results where the curve of "squares" represents the case of $A = 0$, the curve of "circles" represents the case of $A = 0.04$, $T = 240$ and $n = 5$, the curve of "up triangles" represents the case of $A = 0.04$, $T = 60$ and $n = 5$, and the curve of "down triangles" represents the case of $A = 0.04$, $T = 240$ and $n = 10$. We see that for the case of $A = 0$, n_k is proportional to k, confirming the initial distribution of $n_k(0)$. However, for all the other three cases of $A > 0$, n_k is nonlinearly-dependent on k and especially, they are greater than the case of $A = 0$ when $k > 9$. To see the part of $k < 9$ clearly, we let δn_k be the difference between the case of $A = 0.04$, $T = 240$ and $n = 5$ and the case of $A = 0$, see Fig. 7(b). From the inset of Fig. 7(b), we see that δn_k

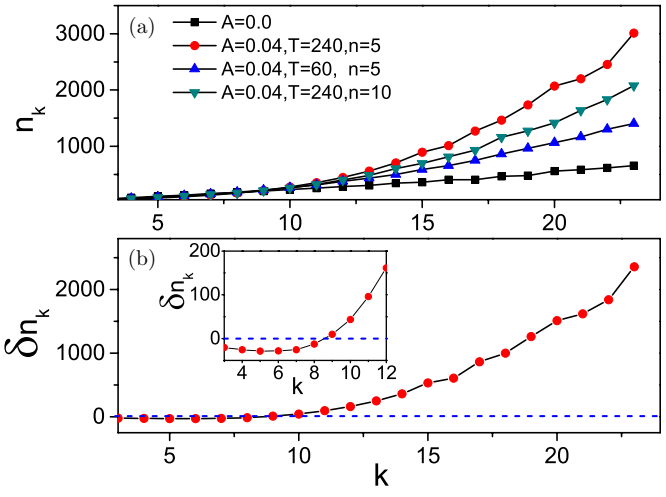

Fig. 7. (Color online) Distribution of agents for the case of maximum congestion (obtained by averaging on 500 realizations), corresponding to the time of $\rho_{\max}$ in Fig. 6. (a) The curve of "squares" represents the case of $A = 0$, the curve of "circles" represents the case of $A = 0.04, T = 240$ and $n = 5$, the curve of "up triangles" represents the case of $A = 0.04, T = 60$ and $n = 5$, and the curve of "down triangles" represents the case of $A = 0.04, T = 240$ and $n = 10$. (b) The difference between the case of $A = 0.04, T = 240$ and $n = 5$ and the case of $A = 0$ where the inset is an amplification of the part of $k < 12$.

is negative in the range of $k < 9$, indicating that the congested agents for $k > 9$ come from the part of $k < 9$.

It is for sure that the nonlinear distribution of n_k in Fig. 7 will induce a nonlinear distribution of infected agents. Figure 8 shows the results where $n_{k,I}$ and $n_{k,S}$ represent the infected and susceptible agents at a node with degree k. From Fig. 8, it is clear that $n_{k,I}$ of all the three cases with $A > 0$ are larger than that of the case with $A = 0$ for $k > 9$, confirming that the congestion at those nodes with $k > 9$ is the direct reason to induce $\rho_{\max}$ in Fig. 6.

We have to point out that it is not linear for more accumulated agents to make more infected agents but nonlinear. To make this point clearer, we simplify the problem to a *star* configuration, a special structure that grasps the main property of SF networks, namely, the role of hubs. The star graph is composed by a central node (the hub) and k peripheral nodes. Each of the peripheral nodes connects solely to the hub. Thus, the connectivity of the peripheral nodes is $k_i = 1 (i = 1, \ldots, k)$ while that of the hub is $k_h = k$. In the congestion phase, the agents at the hub will increase while the agents at the peripheral nodes will decrease, which gives

$$\begin{aligned} n_i(t+1) &= n_i(t) - \alpha A, \quad i = 1, 2, \ldots, k \\ n_h(t+1) &= n_h(t) + \alpha k_h A, \end{aligned} \tag{11}$$

where α is a coefficient. The lost infected agents at a peripheral node from the part $-\alpha A$ will be proportional to $\alpha A[1 - (1 - \lambda)^{n_{i,I}}]$ with $n_{i,I}$ being the infected agents at

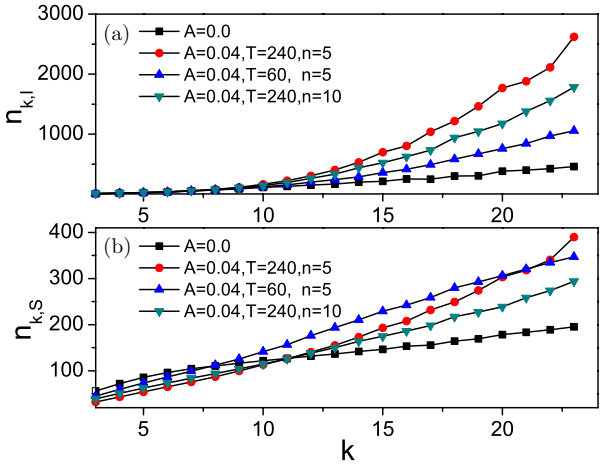

Fig. 8. (Color online) (a) and (b) represent the distributions of infected and susceptible agents, respectively, corresponding to Fig. 7, where the curve of "squares" represents the case of $A = 0$, the curve of "circles" represents the case of $A = 0.04$, $T = 240$ and $n = 5$, the curve of "up triangles" represents the case of $A = 0.04$, $T = 60$ and $n = 5$, and the curve of "down triangles" represents the case of $A = 0.04$, $T = 240$ and $n = 10$. The results are obtained by averaging on 500 realizations.

a peripheral node, and thus the total lost infected agents at all the peripheral nodes are proportional to $k\alpha A[1-(1-\lambda)^{n_{i,I}}]$. Similarly, the gained infected agents at the hub from the part $\alpha k_h A$ will be proportional to $\alpha k_h A[1-(1-\lambda)^{n_{h,I}}]$ with $n_{h,I}$ being the infected agents at the hub. As $n_{h,I}$ is much lager than $n_{i,I}$, the gained infected agents will be greater than the lost infected agents, resulting in a net increase of infected agents proportional to A. The larger T and smaller n will make the congested time longer and thus produce more net increase of infected agents. This is the reason why the $\rho_{\max}$ in Fig. 6 increases with the three key parameters A, T and $1/n$.

5. Discussions and Conclusions

Equation (3) is the first model to describe the effect of periodic rush hours in traffic and can be used to the cases of different traffic such as bus, car, subway, train station, airport, etc. Except the daily and weekly periodicity, these places usually have serious traffic congestion in holidays, especially in the spring festivals of China and Korea. This congestion enhanced epidemic spreading has been evidenced by the common observation that there are more infected people during the holidays than weekdays.

This model of Eq. (3) is only the starting part to study the influence of rush hours on epidemic spreading. A variety of modified Eq. (3) can be considered in the near future such as replacing Eq. (3) by a sinusoidal or even an irregular curve. On the other hand, a road congestion will usually not keep a constant diffusion rate but often decrease until zero. Thus, a deeper consideration should include the reduced diffusion rate in the congestion process.

In conclusion, we have presented a framework to describe the influence of periodic traffic congestion to epidemic spreading. This framework has considered the spatio-temporal features of human activities such as rush hours, objective traveling and a periodic varying diffusion rate, and can be used to different traffic congestions. Numerical simulations show that there are three key parameters, i.e. the amplitude A, period T and duration n to influence epidemic spreading in periodic traffic congestion. Based on the star graph, a theoretical analysis is presented to explain the numerical results. These findings suggest that controlling the contagion in daily traffic congestion may be another effective way to reduce epidemic spreading.

Acknowledgments

This work was partially supported by the NNSF of China under Grant Nos. 11135001 and 11375066, Joriss Project under Grant No. 78230050, and 973 Program under Grant No. 2013CB834100. Y. Do was supported by Basic Science Research Program of the Ministry of Education, Science and Technology under Grant No. NRF-2013R1A1A2010067.

References

1. G. Bianconi and A.-L. Barabasi, *Phys. Rev. Lett.* **86**, 5632 (2001).
2. J. D. Noh, G. M. Shim and H. Lee, *Phys. Rev. Lett.* **94**, 198701 (2005).
3. J. D. Noh, *Phys. Rev. E* **72**, 056123 (2005).
4. M. Tang, Z. Liu and J. Zhou, *Phys. Rev. E* **74**, 036101 (2006); M. Tang and Z. Liu, *Physica A* **387**, 1361 (2008); M. Tang, Z. Liu, X. Zhu and X. Wu, *Int. J. Mod. Phys. C* **19**, 927 (2008); M. Tang, Z. Liu and B. Li, *Chaos* **20**, 043135 (2010).
5. R. Guimera, A. Diaz-Guilera, F. Vega-Redondo, A. Cabrales and A. Arenas, *Phys. Rev. Lett.* **89**, 248701 (2002).
6. G. Yan, T. Zhou, B. Hu, Z. Q. Fu and B. H. Wang, *Phys. Rev. E* **73**, 046108 (2006).
7. P. Echenique, J. Gomez-Gardenes and Y. Moreno, *Phys. Rev. E* **70**, 056105 (2004).
8. P. Echenique, J. Gomez-Gardenes and Y. Moreno, *Europhys. Lett.* **71**, 325 (2005).
9. Z. Y. Chen and X. F. Wang, *Phys. Rev. E* **73**, 036107 (2006).
10. Z. Liu, W. Ma, H. Zhang, Y. Sun and P. M. Hui, *Physica A* **370**, 843 (2006).
11. H. Zhang, Z. Liu, M. Tang and P. M. Hui, *Phys. Lett. A* **364**, 177 (2007).
12. X. Zhu, Z. Liu and M. Tang, *Chin. Phys. Lett.* **24**, 2142 (2007).
13. L. Zhao, K. Park and Y.-C. Lai, *Phys. Rev. E* **70**, 035101(R) (2004).
14. M. Tang, Z. Liu, X. Liang and P. M. Hui, *Phys. Rev. E* **80**, 026114 (2009).
15. J. Candia, M. C. Gonzalez, P. Wang, T. Schoenharl, G. Madey and A.-L. Barabasi, *J. Phys. A* **41**, 224015 (2008).
16. M. Starnini, A. Machens, C. Cattuto, A. Barrat and R. Pastor-Satorras, *J. Theor. Biol.* **337**, 89 (2013).
17. A. Vazquez, B. Racz, A. Lukacs and A.-L. Barabasi, *Phys. Rev. Lett.* **98**, 158702 (2007).
18. L. Hufnagel, D. Brockmann and T. Geisel, *Proc. Natl. Acad. Sci. USA* **101**, 15124 (2004).
19. V. Colizza, A. Barrat, M. Barthelemy and A. Vespignani, *Proc. Natl. Acad. Sci. USA* **103**, 2015 (2006).
20. F. C. Coelho, O. G. Cruz and C. T. Codeco, *Source Code Biol. Med.* **3**, 3 (2008).

21. D. Balcan, V. Colizza, B. Goncalves, H. Hu, J. J. Ramasco and A. Vespignani, *Proc. Natl. Acad. Sci. USA* **106**, 21484 (2009).
22. Z. Ruan, M. Tang and Z. Liu, *Eur. Phys. J. B* **86**, 149 (2013); Z. Ruan, P. M. Hui, H. Q. Lin and Z. Liu, *Eur. Phys. J. B* **86**, 13 (2013).
23. S. Meloni, A. Arenas and Y. Moreno, *Proc. Natl. Acad. Sci. USA* **106**, 16897 (2009).
24. C. Nicolaides, L. Cueto-Felgueroso, M. C. Gonzalez and R. Juanes, *PLoS ONE* **7**, e40961 (2012).
25. D. Brockmann and D. Helbing, *Science* **342**, 1337 (2013).
26. M. Kurant and P. Thiran, *Phys. Rev. E* **74**, 036114 (2006).
27. W. Li and X. Cai, *Phys. Rev. E* **69**, 046106 (2004).
28. W. Jung, F. Wang and H. E. Stanley, *Europhys. Lett.* **81**, 48005 (2008).
29. C. von Ferber, T. Holovatch, Yu. Holovatch and V. Palchykov, *Eur. Phys. J. B* **68**, 261 (2009).
30. M. Catanzaro, M. Boguna and R. Pastor-Satorras, *Phys. Rev. E* **71**, 027103 (2005).
31. R. Pastor-Satorras and A. Vespignani, *Phys. Rev. Lett.* **86**, 3200 (2001).
32. R. Pastor-Satorras and A. Vespignani, *Phys. Rev. E* **63**, 066117 (2001).
33. Y. Moreno, J. B. Gomez and A. F. Pacheco, *Phys. Rev. E* **68**, 035103 (2003).
34. Z. Liu, *Phys. Rev. E* **81**, 016110 (2010).
35. M. E. J. Newman, *Phys. Rev. Lett.* **95**, 108701 (2005).
36. M. A. Serrano and M. Boguna, *Phys. Rev. Lett.* **97**, 088701 (2006).
37. R. Parshani, S. Carmi and S. Havlin, *Phys. Rev. Lett.* **104**, 258701 (2010).
38. M. Tang, Z. Liu and B. Li, *Europhys. Lett.* **87**, 18005 (2009).
39. N. Masuda, *New J. Phys.* **12**, 093009 (2010).
40. V. Colizza, R. Pastor-Satorras and A. Vespignani, *Nature Phys.* **3**, 276 (2007).
41. V. Colizza and A. Vespignani, *Phys. Rev. Lett.* **99**, 148701 (2007).
42. A. Baronchelli, M. Catanzaro and R. Pastor-Satorras, *Phys. Rev. E* **78**, 016111 (2008).
43. Z. Ruan, M. Tang and Z. Liu, *Phys. Rev. E* **86**, 036117 (2012).
44. S. Boccaletti, V. Latora, Y. Moreno, M. Chavez and D.-U. Hwang, *Phys. Rep.* **424**, 175 (2006).
45. K.-I. Goh, B. Kahng and D. Kim, *Phys. Rev. Lett.* **87**, 278701 (2001).
46. M. Barthélemy, *Eur. Phys. J. B* **38**, 163 (2003).